Numerical-Optimal-Control-Compliant Muscle Model for Electrically Evoked Contractions

Tiago Coelho-Magalhães, Christine Azevedo-Coste and François Bailly

***Abstract*—In this paper, an existing physiological muscle model that predicts muscular force in response to electrical stimulation is adapted to be compatible with gradient-based optimization, in particular with numerical optimal control/estimation problems. The objective is to integrate biomechanical models with those that correlate muscle force generation with electrical pulses from a physiological perspective, with the aim of achieving optimal stimulation patterns in activities assisted by functional electrical stimulation. To this end, the activation dynamics of the original model, initially constrained to a stimulation train of predefined and constant length, is reformulated to account for stimulation sequences that dynamically change over time. This is typically necessary to simulate complex motions, which would otherwise be impossible to achieve with the earliest formulation. To identify the model parameters, experimental torque data of 3 participants with spinal cord injury performing electrically evoked isometric quadriceps contractions at different knee angles are used. We then employ an optimal control framework to demonstrate the model's ability to predict knee torques and the possibility of achieving optimized stimulation patterns in simulation for controlling muscle force and knee extension. Our results reveal that the identified model allows accurate prediction of knee torque and optimization of stimulation patterns while satisfying the system's dynamics at the skeletal and physiological muscle levels. This proof of concept is a first step towards physiological muscle model-based control of functional electrical stimulation to achieve movements that best exploit an individual's physiological and biomechanical characteristics.**

***Index Terms*—Biomechanics, musculoskeletal model, functional electrical stimulation, numerical optimal control, simulation.**

I. Introduction

PEOPLE affected by spinal cord injury (SCI) or other neurological conditions that induce limb paralysis may benefit from the use of functional electrical stimulation (FES) to assist them in achieving various functional activities such as grasping, walking, cycling, standing and transfers [1]. However, prolonged application of FES is often limited due to the low selectivity of surface electrical stimulation and the rapid onset of muscle fatigue caused by the non-physiological nature of electrically evoked contractions [2]. Furthermore, inefficient stimulation patterns (i.e., stimulation intervals, pulse duration, amplitude and frequency) result in non optimal recruitment of muscle groups, leading to a lack of synergistic and antagonistic joint control that aggravates the problem of muscle redundancy when reproducing complex movements [3].

T. Coelho-Magalhaes, C. Azevedo-Coste and F. Bailly are with CAMIN team from the National Institute for Research in Digital Science and Technology (INRIA), University of Montpellier, Montpellier, France (e-mails: tiago.coelho-magalhaes@inria.fr, christine.azevedo@inria.fr and francois.bailly@inria.fr).

To overcome these limitations, some studies have combined FES-stimulated muscle dynamics and biomechanical models with optimal control methods to predict the causal relationship between electrical stimulation of muscles and joint motion [4]. This integration employs diverse optimization criteria, in which a user-defined cost function is minimized to compute control signals over a finite time horizon using numerical techniques. It can include the total number of muscles stimulated and the corresponding activation levels necessary to achieve a desired trajectory, whose solution can potentially mitigate the adverse effects of muscle fatigue. In [5] and in [6], musculoskeletal models and dynamic optimization were employed to determine the muscle activation sequence needed to reproduce in simulation the human walking based on reference trajectories obtained from the gait of able-bodied subjects. The optimal control solution was determined by minimizing the tracking error of joint angles and the simultaneous activation of agonist and antagonist muscles. Real experiments were further explored in [7], where the muscle activation patterns obtained were used as a basis for real-time stimulation control during FES-assisted walking of subjects with SCI, allowing superior performance compared to manual or open-loop approaches in terms of energy cost and walking speed. A similar approach was investigated in [8], where, in addition to the lower extremity joints trajectories, objectives aimed to minimize the high upper body effort required during walker-assisted standing and walking. Hybrid FES-exoskeleton systems have also demonstrated the potential to assist SCI people while completing tasks that require highly coordinated movements based on model predictive control [9]–[11].

Although the above studies revealed an effective combination between optimal control and FES-assisted activities, they relied on the simplifying assumption that muscle activation can be directly assimilated to stimulation output, which avoided the need to model complex excitation-contraction dynamics, despite the fact that some have employed fiber recruitment curves as a proxy to model the relationship between electrical stimulation and the neuromuscular system [6], [7], [9], [10]. Consequently, the phenomenological approach behind the muscle activation models commonly employed in FES-driven simulations still lacks physiological realism.

From a physiological perspective, a variety of models have been advanced to explain the interaction between electrical stimulation and muscle force dynamics [12]. The muscle model proposed by Ding *et al.* [13]–[15] describes how electrical pulses trigger muscle activation by modeling the formation of the calcium-troponin complex, which initiates cross-bridge cycling - the actin-myosin interaction leading to

force generation. Compared to alternative models, it has fewer parameters that require identification (see [16], [17]), which reduces the complexity associated with its implementation. It was validated with individuals with SCI [18], [19] and was suggested to be the most accurate model to predict muscle force outputs from both trained and untrained paralyzed limbs [20]. It accurately predicted force under non-isometric [21], [22], and fatigued conditions [23]–[25]. This model has been investigated in optimal control problems to track a reference force, focusing on the optimized stimulation frequency to achieve a desired force and the maximization of the final force response [26], [27]. In [28], Ding *et al.* model was used in dynamic optimization problems to investigate the effects of an optimal sequence of stimulation pulses required to maintain a desired isometric contraction while minimizing muscle fatigue. Their results suggested that muscle fatigue was lower using an optimized-frequency pulse train rather than a constant-frequency one while producing equivalent force-time integrals.

Although they demonstrated the possibility to optimize the force control of a single physiological muscle model through FES efficiently, these investigations were not accounting for the musculoskeletal dynamics, making it impossible to conclude on the possibility of using such a physiological muscle model in a biomechanical task prediction. Furthermore, these investigations present two limiting factors related to the activation dynamics: i) the original formulation of the model includes a summation that increases in size as the stimulation duration extends and ii) it is computed with respect to a stimulation train of predefined and constant length. These characteristics hinder the efficient implementation of optimization-based motion predictions with FES-driven musculoskeletal models. This is mainly due to the nature of direct transcription methods, which are necessary to transform continuous trajectory optimization problems into generic discrete nonlinear programs (NLP's), such as direct collocation or multiple shooting [29]. Limitation i) which results in a change in the summation size at each shooting node, would necessitate to systematically work with multiphase problems, degrading the computational performances of the approach. Limitation ii) implies that it is not possible to let the numerical solver turn the stimulation on and off at arbitrary instants, as required in complex motions. Instead, this original formulation restricts optimization sequences to really simple scenarios in which the muscle stimulation is always turned on and for a predefined duration.

With the aim of making the predictive capabilities of Ding *et al.* model compatible with optimized FES-driven motions, we noticed that the effects of past electrical pulses are negligible as a result of the exponential decay present in the activation dynamics formulation, notably in the summation effect associated with the rate-limiting steps leading to the formation of the Ca^{2+}-troponin complex. Hence, we hypothesized that a limited subset of successive pulses would be sufficient for the calculation of the resulting evoked-muscle force and thus simplifying the formulation and the solving of the OCP.

That being said, a key contribution of this paper is the reformulation of Ding *et al.* model to make it compatible with gradient-based optimization and, in particular, numerical optimal estimation/control problems. We also evaluate the impact of this approximation on computational performance, including the time to convergence and the number of nonlinear programming iterations needed to solve the problem. Experimental data from isometric evoked contractions of the quadriceps muscles for different knee extension angles are collected from individuals with SCI to identify model parameters and compare with the prediction of knee torque in simulation. Finally, we demonstrate the feasibility of implementing trajectory optimization with our adapted FES-activated muscle model to optimize the knee joint trajectory using numerical optimal control[1].

This preliminary evaluation using a complete musculoskeletal optimization-based motion prediction, including the formulation of trajectory optimization problems, is a requisite step in the process of further investigating the potential of using this physiological muscle model in real-time applications, in which model-based optimization of the control laws represents a promising way for achieving more versatile movements in response to electrical stimulation.

II. Methods

The workflow depicted in Fig. 1 offers a comprehensive overview of the methodological framework, which will be elaborated in greater detail subsequently.

A. Muscle-force model

The physiological-based muscle model proposed in [13] consists of two coupled differential equations. They relate the dynamics of the rate-limiting step that leads to the formation of the Ca^{2+}-troponin complex (c_N; unitless) to the force development as a response to n consecutive electrical pulses delivered before time t.

This study presents a novel dynamic formulation that captures the temporal influence of a finite number of pulses p moving in time — a feature crucial for its integration with numerical optimal control and estimation problems — marking a distinct advancement over earlier models. We define $n(t) = \lfloor t/T \rfloor$ to represent the largest integer n, such that $n \leq t/T$, where T represents a constant pulse period. Therefore, the activation dynamics is approximated by:

$$\frac{dc_N}{dt} = \frac{1}{\tau_c} \sum_{i}^{n(t)} \alpha_i R_i \exp\left(-\frac{t - t_i}{\tau_c}\right) - \frac{c_N(t)}{\tau_c}, \qquad (1)$$

where $i = max(1,\ n(t) - p)$ is within the truncated or window-sized train of pulses containing the history of the last $p \in \mathbb{N}^*$ pulses. The states *on, off* of each pulse is represented by $\alpha_i = \{0, 1\}$ at the time of the ith pulse, where $t_i = iT$. The parameter R_i accounts for the nonlinear summation of the c_N transient upon the time response $\tau_c(ms)$ - a constant controlling the rise and decay of c_N -, which is given by:

$$R_i = \begin{cases} 1 & if\ i = 1, \\ 1 + (R_0 - 1)\exp(-\frac{t - t_i}{\tau_c}) & if\ i > 1, \end{cases} \qquad (2)$$

[1]https://github.com/pyomeca/bioptim

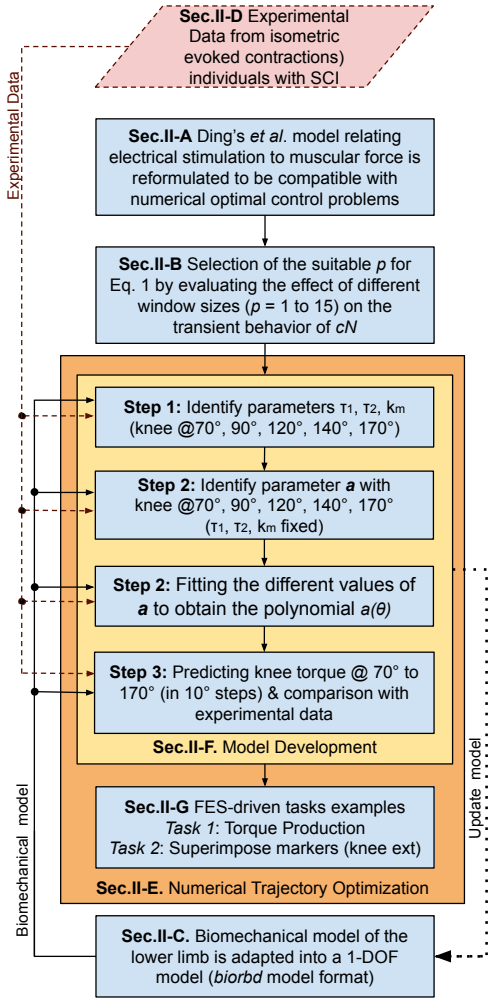

Fig. 1. Workflow representation of the methodology proposed. The muscle model is adapted for numerical optimal control, where key parameters are identified using knee torque data from SCI subjects across multiple knee angles. Then, the model is validated by predicting knee torque and applied to optimize FES-driven tasks. The respective sections are indicated accordingly.

where R_0 (unitless) represents the magnitude of enhancement in c_N [14]. The evolution of Ca^{2+}-troponin complex c_N is related to the instantaneous force F(N) through the Michaelis–Menten functions defined by:

$$m_1(t) = \frac{c_N(t)}{K_m + c_N(t)}, \tag{3a}$$

$$m_2(t) = \frac{1}{\tau_1 + \tau_2 m_1(t)}, \tag{3b}$$

where K_m is the sensitivity parameter of strongly bound cross-bridges to c_N, $\tau_1(ms)$ is the time constant of force decline in the absence of strongly bound cross-bridges and $\tau_2(ms)$ is the time constant of force decline due to friction between actin and myosin [30]. These functions are part of the muscle force dynamics:

$$\dot{F} = m_1(t)A(pd, \theta) - m_2(t)F(t), \tag{4}$$

where F represents the mechanical force derived from a linear spring, a damper, and a motor in series [14]. The force output $F(t)$ is ultimately parameterized by one function (A) and five parameters (τ_1, τ_2, τ_c, K_m, and R_0).

Finally, we assumed that muscle force could be influenced by modulating A as a function of the stimulation pulse duration as in [19] and by the knee angle as in [30]:

$$A(pd, \theta) = a(\theta)(1 - \exp(-(pd - pd_0)/pd_t)), \tag{5}$$

where $a(\theta)$ represents a force scaling factor accounting for muscle length, thus depending on the knee joint angle θ. The parameter $pd(\mu s)$ refers to pulse duration, $pd_0(\mu s)$ represents the threshold offset that characterizes the muscle sensibility to the pulse intensity and $pd_t(\mu s)$ describes how the scaling parameter varies with the increasing of pulse duration [19].

B. Data Analysis of the truncation method

In (1), the existing exponential term causes the effect of each pulse to decrease over time. In this case, the number of previous pulses (in relation to the actual time) that actually have an effect on the instantaneous activation dynamics could be defined by approximating the model. To define the window size (parameter p related to (1)) that would be suitable for the simulations proposed in this work, we quantitatively evaluated the truncated method with window sizes ranging from 1 to 15 on a random pulse train for stimulation frequencies ranging from 25 to 100 Hz in 5 Hz steps. To this end, we used the analytical solution for the transient behavior of c_N presented in [13] to calculate the root mean square error (RMSE) between the different window sizes (1-15) and a window of size 20, which provided equivalent results to the original model while being compatible with our optimal control framework. The average values of the parameters τ_1, τ_2 and K_m from [19] were used in the calculation. Fig. 2 illustrates the resulting approximation of (1) using the different sizes for p for a random pulse train for a frequency of 40 Hz.

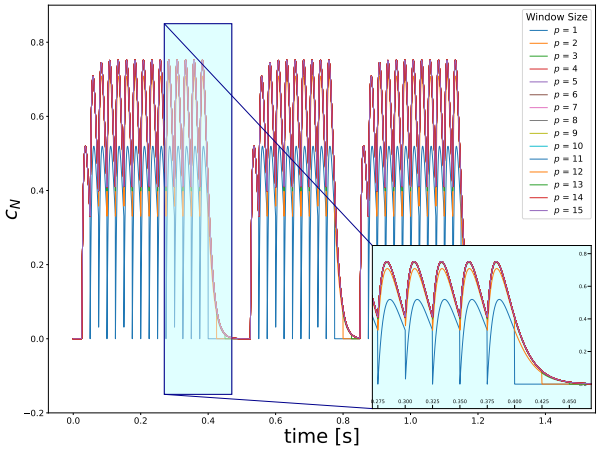

Fig. 2. Effects of the different window sizes (p = 1 to 15) on the approximated response of c_N for a 40 Hz stimulation frequency.

C. Biomechanical model

We adapted an existing lower limb model[2] to a 1-degree-of-freedom (DOF) model using the OsimToBiomod library

[2]https://simtk.org/projects/cycling_sim

converter[3] (Fig. 3). The biomechanical model was simplified to have one right leg with four muscles (*rectus femoris*, *vastus lateralis*, *vastus medialis* and *vastus intermedius*) to simulate the quadriceps femoris muscle under isometric electric-evoked contractions. The model also defines the constraints concerning joint range of motion and muscle characteristics and was used in both the parameter identification procedures (Section II-F) and FES-induced tasks (Section II-G).

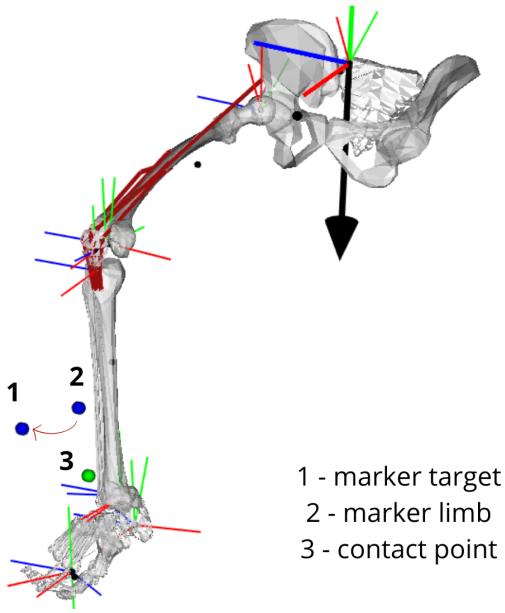

Fig. 3. Biomechanical model of the right lower limb. The blue markers should be superimposed on the knee extension task: marker #1 is the target to be reached by marker #2. The green marker (#3) is a contact point used to lock the limb during isometric contractions.

D. Experimental Data

We used experimental data from a previous study of our team [31] to identify the model parameters and to validate this identification on the prediction of knee-joint torques. Measurements were obtained during isometric evoked contractions of the quadriceps femoris muscles from the two legs of three male participants with SCI (42.4 ± 6.9 years and body mass index of 26.6 ± 2.9). The study protocol received approval from the Ethics and Research Committee of the Faculty of Ceilandia at the University of Brasília, Brasília, Brazil (CAAE: 09303218.6.0000.8093, Ethical Approval number 3.632.981). All procedures were performed in accordance with the ethical standards of the 1964 Declaration of Helsinki and its later amendments. Written consent was obtained from each participant. Measurements were conducted using an isokinetic dynamometer (Biodex Medical Systems, NY, United States). The movement patterns to control the dynamometer and data acquisition are detailed in [31]. Stimulation pulses were delivered to participants using the FESBox 4 stimulator (BerkelBike B.V., Netherlands).

To identify the model's parameters in this work (see Section II-F), we used the experimental data from the following procedures: maximal evoked contractions (MEC), and torque to knee extension angle relationships (here, referred to as LEN due to its relationship with muscle length). In all scenarios, the stimulator delivered symmetric, rectangular, biphasic pulses with a phase-width of 400 μs, and constant frequency trains (CFT) at 40 Hz. The MEC measurements accounted for three short (500 ms) isometric contractions at a knee angle of 90° with a stimulation amplitude of 120 mA. Between consecutive contractions, a resting period of 1 min was included to allow for full recovery of the neuromuscular system. The LEN setup accounted for two short (500 ms) isometric contractions for each angles, ranging from 70° to 170° in 10° steps. Contractions were performed every 30 seconds to allow the muscles to rest between them. The stimulation intensity was adjusted to produce a peak-torque of approximately 40% of the MEC at the lowest knee angle (i.e. 70° knee extension angle). In the following, we considered a full knee extension to be reached at 180° whereas lower values indicate a knee flexion to keep the same formalism as in [31].

We used data from the conventional configuration (CONV) described in [31], where two electrodes of same size (68×125 mm, bipolar stimulation) were placed proximal and distally on the quadriceps muscle. Each testing session was divided into two parts and performed for both the left and right legs individually during the same session.

E. Trajectory Optimization Formalism

Whether to identify the model parameters (estimation) or to control the model in simulation (control), we used the numerical trajectory optimization framework implemented in [32], a Python framework for biomechanical optimal control that handles musculoskeletal models. The problems were solved using IPOPT with exact Hessian [33], and CasADi for algorithmic differentiation [34]. For a system whose dynamics is governed by an ordinary differential equation of the form $\dot{\mathbf{x}} = \mathbf{f}(\mathbf{x}, \mathbf{u})$, with $\mathbf{x}$ and $\mathbf{u}$ the state and control vectors, a generic trajectory optimization problem can be written as:

$$\min_{\mathbf{x}(t),\mathbf{u}(t),\mathbf{p}} = J(\mathbf{x}(t), \mathbf{u}(t), \mathbf{p}) \tag{6a}$$

$$\text{s.t.} \quad \forall t,\ \dot{\mathbf{x}} = \mathbf{f}(\mathbf{x}(t), \mathbf{u}(t), \mathbf{p}) \tag{6b}$$

$$\forall t,\ \mathbf{g}(\mathbf{x}(t), \mathbf{u}(t)) \leq 0 \tag{6c}$$

$$\mathbf{x}(0) = \mathbf{x_0} \tag{6d}$$

with J the cost function, $\mathbf{p}$ a vector of model parameters and $\mathbf{x_0}$ the initial state. The inequality constraints are gathered in function $\mathbf{g}$. To be numerically tractable, this continuous-time optimization problem is transcribed into a finite-dimensional nonlinear program using the multiple shooting approach implemented in [32]. The goal is to find the control input $\mathbf{u}(t)$, the states $\mathbf{x}(t)$, and the parameters $\mathbf{p}$ minimizing the cost function defined for each phase while satisfying the dynamic and boundary constraints introduced in (6). In the following, the control input $\mathbf{u}(t)$ corresponds to the pulse duration ($\mathbf{pd}(t)$); the states $\mathbf{x}(t)$ includes $\mathbf{c_N}(t)$ and force $\mathbf{F}(t)$ for each muscle, the knee joint position $\mathbf{q}(t)$ and velocity $\dot{\mathbf{q}}(t)$, and the history of each pulse, represented by $\alpha_\mathbf{i}(t)$ in (1), which is implemented as a vector of size 6, based on the results

[3]https://github.com/pyomeca/osim_to_biomod

obtained from the truncation method analysis (see Section III), whose dynamics was implemented as $\dot{\alpha_i} = (\alpha_i - \alpha_{i-1})/T$, resulting in zero variation when the alpha states remain unchanged, and $-1/T$ or $+1/T$ when the state is deactivated or activated, respectively, within a pulse period.

F. Model Development

The force model for non-fatigued muscles is described with one function $A(pd, \theta)$ and five parameters: R_0, τ_c, τ_1, τ_2, and K_m [19]. In (5), we defined A as a function of θ in a similar approach as presented in [30], and as function of pulse duration $pd(t)$ and parameters pd_0, pd_t as presented in [19]. However, these last two were not considered in the parameter identification processes, and the average values presented in [19] were used in this work. The parameters R_0 and τ_c are fixed at 5 and 11 ms, respectively, as suggested in [19] for the quadriceps femoris muscles of individuals with SCI. Thus, only three parameters and one function remain to be identified for each subject and leg: τ_1, τ_2, K_m and $a(\theta)$. Finally, the following steps were used to identify the model's parameters and obtain predicted torques. The OCP was discretized using 40 shooting nodes per second (one stimulation pulse per node with time in-between nodes corresponding to the pulse period) with a 5-step RK4 integration in-between.

Step 1: *Identification of τ_1, τ_2, and K_m.*
For each subject and each leg, we used experimental torques measured in the MEC and LEN setups at respectively $[90°]$ and $[70°, 90°, 120°, 140°, 170°]$ as input data to our identification problem (Section II-D). We gathered the five torque trajectories containing the first evoked contraction of each previously described configuration in an experimental torque vector $\boldsymbol{\tau_{exp}}$. An optimal estimation problem was formulated to track these experimental torque data by optimizing τ_1, τ_2, K_m and A (4), while satisfying the system's dynamics. Consequently, a problem of the form of (6) was solved with the following equation as a transcription of (6a):

$$\min_{\substack{\mathbf{x}(t),\mathbf{u}(t),\\ \mathbf{p}=[\tau_1,\,\tau_2,\,K_m,\,A]}} \quad \frac{1}{N}\sum_{k=0}^{N-1}(\boldsymbol{\tau}_k^{\boldsymbol{pred}}(A,\ \tau_1, \tau_2, K_m) - \boldsymbol{\tau}_k^{\boldsymbol{exp}})^2 \tag{7}$$

where $\boldsymbol{\tau}^{pred}$ is the torque trajectory predicted by the model, $\boldsymbol{\tau}^{exp}$ is the measured torque trajectory and N is the total number of shooting nodes. As the values of τ_1, τ_2, and K_m are not dependent on θ, the identified values for these parameters are kept fixed in the following steps.

Given the structure of $\boldsymbol{\tau}^{exp}$, the problem implementation was multi-phase, with discontinuous phase transitions to let the model switch from one knee position to another within the same optimization problem (i.e., each phase of the problem represented a distinct knee angle). To enforce isometric contractions during the optimization, the tibia was locked by a non-accelerating contact point at each knee position (Fig. 3, green circle #3). We defined $pd_{max} = 800\mu s$ (same as pulse duration during experiments) and $pd(t)$ to be dependent on the experimental setup (i.e., MEC or LEN) when stimulation was *on*, or 0 otherwise. For instance, $pd(t) = 800\mu s$ for MEC setup and, for LEN, the value was defined to be a percentage of pd_{max} necessary to reproduce the measured torque ratio at $90°$ between LEN and MEC configurations for each subject/leg. The control bounds were set according to the stimulation state (i.e., *on* or *off*) of the experimental data.

Step 2: *Determination of the $a(\theta)$ polynomial.*
We considered τ_1, τ_2, and K_m to be not dependent on θ and these parameters were fixed at the values previously identified. In this step, we defined a to be an optimization parameter and used five contractions from the LEN dataset at $\theta = [70°, 90°, 120°, 140°, 170°]$ to identify $a(\theta)$. This time however, five separate optimal estimation problems were solved for the various knee angles, the joint locking being simulated by a contact point. For each θ value, the problems were formulated to track the experimental torque data by optimizing a, while satisfying the system's dynamics. Consequently, a problem of the form of (6) was solved with the following equation as a transcription of (6a):

$$\min_{\mathbf{x}(t),\mathbf{u}(t),\mathbf{p}=\hat{a}_\theta} \quad J_\theta = \frac{1}{N}\sum_{k=0}^{N-1}(\tau_k^{pred}(\hat{a}_\theta) - \tau_k^{exp})^2, \tag{8}$$

with $\theta = [70°, 90°, 120°, 140°, 170°]$ and $\hat{a}_\theta$ the optimized value of a at angle θ. Finally, $\hat{a}_\theta$ values were fit within a fourth-degree polynomial using a least squares fitting (*numpy.polyfit*) with Python (v3.10.13) to determine an analytical expression for $a(\theta)$.

Step 3: *Prediction of torque and force responses.*
A validation step was then implemented, consisting in a series of simulations with the previously identified model's parameters to evaluate its accuracy to reproduced the isometric evoked-contraction of the LEN dataset (from $70°$ to $170°$ in $10°$ steps). It should be noted that among the eleven knee angles used in this validation step, only five were used in the identification phase (steps 1 and 2), in which the first series of evoked contractions from the LEN dataset was used. The obtained torque trajectories were then compared to the experimental ones from the second series of evoked contraction of the LEN dataset (Section II-D). In this sense, the data used for the identification process are different from those used for prediction. A linear regression was used to determine how well the model predicted the torque-time integrals (TTIs) for each subject by knee angle (see Fig. 7). A perfectly accurate model would have both a slope and the coefficient of determination R^2 of one. The RMSE between the experimental and the predicted torque across all participants and legs are presented with respect to the different knee angles (see Fig. 6). The R^2 and the RMSE values for both legs of participant 1 were also calculated and reported.

G. FES-driven tasks examples

To demonstrate the ability of the adapted physiological muscle model to be used in trajectory optimization problems, we developed a multi-phase optimization problem aiming to achieve six different isometric torque targets at the knee joint

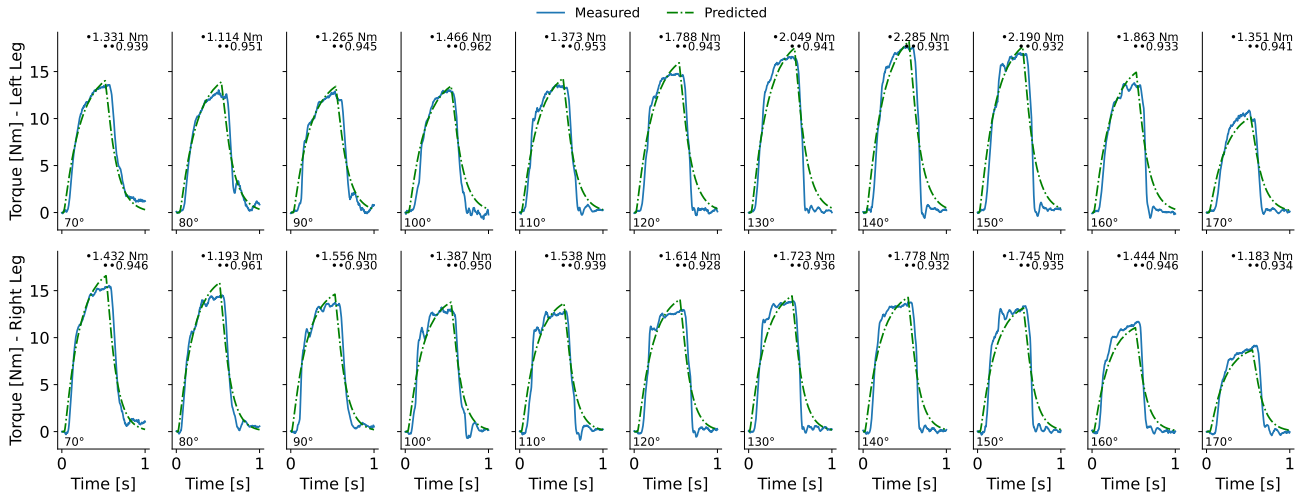

Fig. 4. Measured and predicted torques for both legs of subject 1. RMSE (•) and R^2 (••) are shown for each knee angle.

during the first six phases followed by a knee extension task to superimpose the target (Fig. 3, #1) and shank (Fig. 3, #2) markers. Each phase's objective function is further developed in equations (9) and (10), respectively. For synthesizing the optimal stimulation pattern, pulse duration was optimized as a piecewise constant control variable within $86 - 800\mu s$ at a constant frequency of 40 Hz. In (5), the values of pd_0 and pd_t were considered as the average values presented by [19].

The OCP is therefore subject to multibody dynamics driven by the FES dynamics (1)-(5), as well as path constraints in the domains of $\mathbf{u}$ and $\mathbf{x}$ that include the pulse duration and joint kinematics within their physiological ranges of motion. The OCP was discretized using 40 shooting nodes per phase with a 5-step RK4 integration in-between. Each of the two phases of the problem are detailed separately as follows.

FES-Driven Torque Production Task:
In the first six phases, the objective is to perform isometric contractions with the knee locked at 90° by a contact force (marker 3, Fig. 3) to produce target torques from 5.0 to 30.0 Nm in 5.0 Nm steps. An optimal control problem was formulated to reach the desired torque by optimizing $\mathbf{pd}$ (5), while satisfying the system's dynamics. Consequently, a problem of the form of (6) was solved with the following equation as a transcription of (6a):

$$\min_{\mathbf{x}(t),\mathbf{u}(t)} \sum_{k=0}^{N-1} \Big[\omega_1(\tau_k^{sim} - \tau_k^{target})^2 + \omega_2\ pd_k^2 + \omega_3\ F_k^2 + \omega_4\ q_k^2 + \omega_5\ \dot{q}_k^2\Big], \tag{9}$$

where ω_1=1e4, ω_2=0.1, ω_3=0.1, ω_4=1e3 and ω_5=1e3.

FES-Driven Knee Extension Task:
Following the first six phases, the goal here is to superimpose a limb marker (Fig. 3, marker #1) with a target one (Fig. 3, marker #2) using the biomechanical model of the leg previously described. An optimal control problem was formulated to minimize the distance error between two markers (i.e., superimpose) and the control input $\mathbf{pd}$ (5) while satisfying the system's dynamics. The marker one ($m^{sim} \in \mathbb{R}^3$) was fixed in the limb system of coordinates and the second one ($m^{target} \in \mathbb{R}^3$) fixed in the scene and corresponding to the target marker. A problem of the form of (6) was solved with the following equation as a transcription of (6a):

$$\min_{\mathbf{x}(t),\mathbf{u}(t)} \sum_{k=0}^{N-1} \Big[\omega_1(m_k^{sim} - m_k^{target})^2 + \omega_2\ pd_k^2 + \omega_3\ F_k^2 + \omega_4\ q_k^2 + \omega_5\ \dot{q}_k^2\Big], \tag{10}$$

ω_1=1e5, ω_2=0.1, ω_3=0.1, ω_4=1e3 and ω_5=1e3.

H. Computational performance analysis

Finally, from the results obtained in Section II-B and considering low error obtained on the approximation of c_N dynamics at 40 Hz, we arbitrarily chose nine window sizes (4 to 10, 15 and 20) to report their influence on the computational performance in the two proposed FES-driven tasks: knee extension and torque production. At this time, the evaluation of the performance of these two tasks is carried out separately, in a one-phase only OCP for each, and we defined a target torque of 20 Nm for the latter. The number of iterations and the time to convergence were computed for each of the FES-driven tasks. The RMSE error associated with the approximation of the c_N dynamics when compared to a 20-size window is also evaluated.

III. Results

We modified the model presented in [19] and identified its parameters using experimental data collected from isometric muscle contractions of the quadriceps muscles in individuals with spinal cord injury at different knee angles. First, it was necessary to define the window size appropriate to the truncation proposed in the reformulation of the muscle activation dynamics of the model. Fig. 5 shows the error represented as $\log_{10}$(RMSE) associated with the c_N behavior

TABLE I

COMPUTATIONAL PERFORMANCE ANALYSIS ON TORQUE PRODUCTION AND KNEE EXTENSION TASKS. THE EFFECT OF DIFFERENT WINDOW SIZES (4 TO 10, 15 AND 20) ON THE NUMBER OF NLP ITERATIONS, TIME TO CONVERGENCE, AND c_N RMSE ERROR WHEN COMPARED TO A 20-SIZE WINDOW ARE SHOWN.

Torque Production	4	5	6	7	8	9	10	15	20
NLP iterations	126	128	119	96	109	112	121	166	117
Convergence time [s]	12.87	17.84	28.94	26.4	33.23	39.61	45.23	102.52	96.02
c_N approx. error	$17.01e-5$	$14.79e-6$	$1.23e-06$	$9.92e-08$	$7.57e-09$	$5.49e-10$	$3.76e-11$	0.0	–
Knee Extension Task	4	5	6	7	8	9	10	15	20
NLP iterations	285	219	218	228	262	268	251	284	375
Convergence time [s]	26.14	24.14	48.76	56.46	72.27	87.43	92.06	173.34	339.33
c_N approx. error	$12.63e-5$	$11.82e-6$	$1.05e-06$	$8.92e-08$	$7.07e-09$	$5.26e-10$	$3.67e-11$	$3.11e-14$	–

Tests were conducted on a Intel® Core™ i5-12600H @ 4.5G Hz × 16

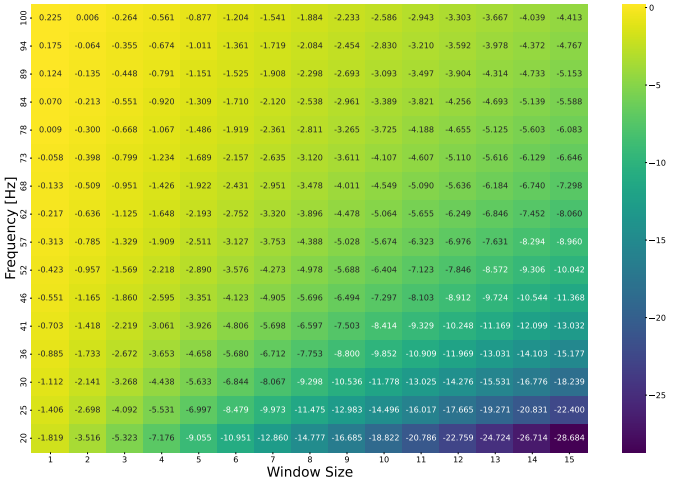

Fig. 5. Error evaluation of the approximation of c_N dynamics. Window sizes from 1 to 15 were compared to a 20-window-size for different frequency values. The values are reported as $\log_{10}$(RMSE).

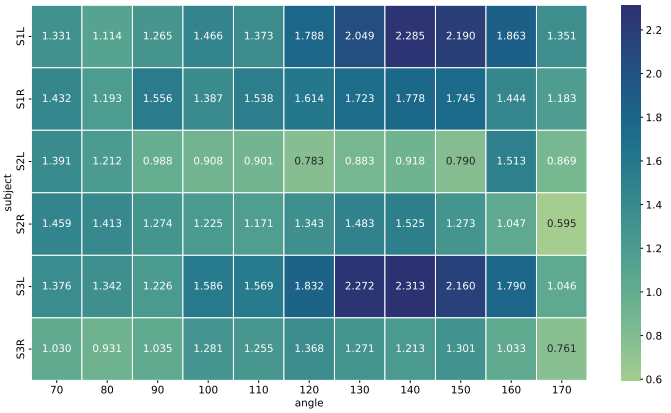

Fig. 6. RMSE between the experimental and predicted knee torques sorted by angle and per subject. Each subject are associated with the respective leg: *R*: right and *L*: left

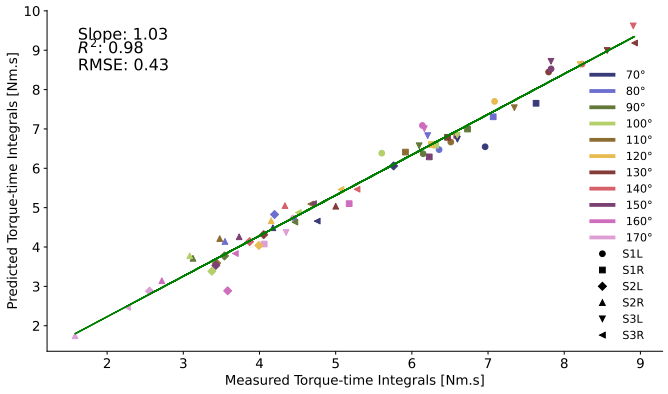

Fig. 7. Measured Torque-time Integrals per subject per angle. Comparison between the predicted and experimental Torque-time Integrals (TTI) plotted for all subjects (and each leg) at each knee angle tested.

when comparing it to a simulation of a 20-size window used in a random stimulation train. For the stimulation frequency used in the experiments (40 Hz), the error associated with a window-size of 6 was of the order of $1e-5$.

Then, using this window size in the model parameter identification process, we obtained the averaged values for τ_1 = 0.1194 ms, τ_2 = 0.1462 ms, K_m = 0.8 and $a(\theta)$ polynomial coefficients [651.9537, 1734.5855, 1136.0953, -325.5792, 216.7115]. The fitting of torque at different knee extension angles for both legs of the first subject is presented in Fig. 4 with the respective values of RMSE and R^2. These results are complemented by Fig. 6, in which the torque RMSE for all subjects is sorted by knee angles. In addition, a comparison of TTIs between experimental and predicted torques and its associated trend line can be seen in Fig. 7. The results show a slope of 1.03, R^2=0.98 and RMSE=0.43 Nm. An overall RMSE of less than 1.0534 Nm was achieved compared to the experimental data.

Window sizes of 4 to 10, 15 and 20 were used during FES-driven tasks to evaluate their impact on computational performances. Table I shows the number of NLP iterations, the time to convergence in IPOPT, and the RMSE error associated with the c_N approximation compared to a 20-window size for each task separately. Considering the order of error achieved by a 6-size window ($p = 6$) (order of 1e-6) and the time to convergence, we considered this size suitable to be used in the model development. With this approximation being compared against $p = 20$, the adapted model with $p = 6$ reduces the convergence time by up to 30.14% and 14.37% during the torque production and knee extension tasks, respectively. The absolute number of NLP iterations was considerably reduced in the latter (by 58.13%) but no improvement was observed in torque production with respect to this indicator. Another important aspect to consider is the time per iteration, which

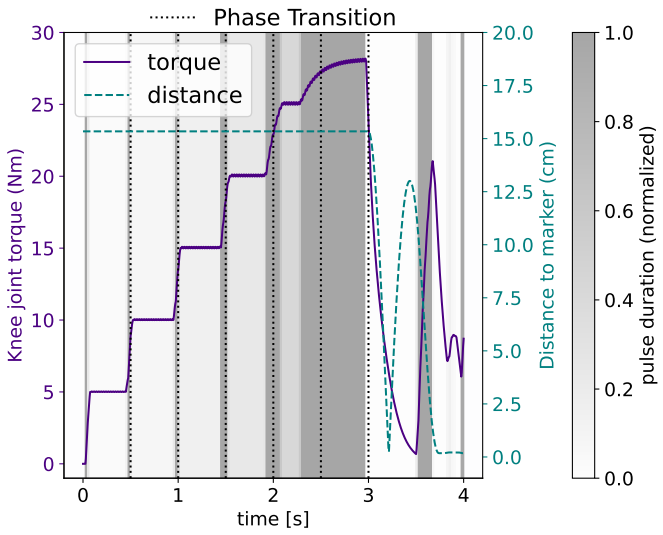

Fig. 8. Biomechanical tasks outcomes: the optimized knee torque and the distance between markers from a multi-phase problem. In the first six phases, the goal is to reach torque targets varying from 5.0 to 30.0 Nm in 5.0 Nm steps as a result of the isometric contraction of the quadriceps muscle (continuous line). In the last phase, the leg is allowed to move freely and the goal is to minimize the distance between target and limb markers by optimizing the leg position (dashed line). The transition between phases are indicated in the vertical lines. Optimized pulse duration is presented in a background gradient scale, with the normalized value indicated.

was considerably reduced in both tasks.

Finally, Fig. 8 presents the optimized knee torque and distance between markers over time in the proposed multi-phase problem. The optimized pulse duration is presented in a background gradient scale, with the normalized value indicated. In the first six phases, the target torques varying from 5.0 Nm to 30.0 Nm in 5.0 Nm steps are successfully reached and then controlled during this period except from the 6^{th} phase, where the pulse duration was saturated and the model was not able to achieve the proposed torque. It is worth noting that the distance between the target and limb markers (markers 1 and 2 in Fig. 3) remains the same throughout this period as a result of isometric contraction of the quadriceps muscle. In the last phase, the leg is allowed to move freely aiming to align the two markers and the final distance between them is reduced to 1.81 mm.

IV. Discussion

In this study, we adapted an existing mathematical model able to predict skeletal muscular force in response to electrical stimulation [13]–[15] making it compliant with optimal control/estimation problems. The original formulation of the activation dynamics relied on the summation of a fixed number of exponentially decaying responses to stimulation pulses within a predefined stimulation period. We hypothesized the effects of past electrical pulses on the activation dynamics could be neglected in the course of time without degrading the model's ability to predict muscle force. In this sense, by restricting the summation to a limited number of terms (or pulse responses) within a moving window preceding time t, the model could approximate non-fixed stimulation periods.

To evaluate this approach, we assessed the impact of using different window sizes (4–10, 15, and 20 terms) on the activation dynamics computation error and computational performance. We observed that adequate window sizes can result in low approximation errors while reducing the time to convergence and the number of NLP iterations to solve OCP as demonstrated in Table I. Consequently, an evaluation was performed to determine the efficacy of the model in predicting muscle force.

To identify the parameters of the model and predict the knee torques, we used experimental torque data from isometric contractions of the quadriceps muscles of individuals with SCI at different knee angles. Similarly to the parabolic approach presented in [30], we implemented a fourth-order fitting polynomial ($\alpha(\theta)$) to capture the influence of the force-length relationship associated with the knee extension angle on the resulting joint torque. The identified model was able to successfully estimate the peak torque at the different knee positions as there was no pulse duration control at this point (pulse duration was constant during knee-torque prediction) and the polynomial-dependency to $\alpha(\theta)$ was supposed to capture the different peak torques at this point. For visual inspection, Fig. 4 shows how well our model fits the experimental torques at various angles, in accordance with the results presented in [31]. Although no significant differences were indicated, the abrupt drop in torque observed during experimental measurements (especially when higher peak-torques are achieved) contributed to greater values of RMSE. These results are complemented with Fig. 6, in which the torque RMSE for all subjects is sorted by knee angle, and with the TTI evaluation shown in Fig. 7. Despite the fact that we do not directly assess muscle force, but rather the actual torque produced, our findings suggest a better precision compared to what was found in [30]. These results support our initial hypothesis that the reduced window sizes did not degrade the ability of the model to predict muscle forces while being compatible with simulations that require more complex stimulation patterns.

We then demonstrated the feasibility of using our adapted model by formulating trajectory optimization problems to simulate two biomechanical tasks including knee extension and torque production tasks using numerical optimal control. For that, in addition to the influence of $\alpha(\theta)$, our model was adapted to account for the effect of pulse duration as a control input as suggested in [19]. Note that it could be further extended to include pulse amplitude, which is frequently used in control strategies for FES [35], by adapting the activation dynamics formulation (1), as already demonstrated to be possible [36]. As illustrated in Fig. 8, in the initial six phases of a multi-phase problem, the objective of attaining different knee torques resulting from isometric contraction of the quadriceps muscle was not only accomplished but remained controlled throughout the duration of the phases, with the exception of the final one, wherein the maximum isometric forces achieved by the muscle model was not sufficient to attain the expected target torque of 30.0 Nm. In the last phase, we defined the objective of minimizing the distance between the two markers by optimizing the position of the leg as a result of

the muscle contractions, which resulted in a final distance of 1.81 mm. Although we did not validate FES-driven motions experimentally, our model demonstrated potential to be used in simulation and its compatibility with trajectory optimization problems.

A limitation of this work is that we did not identify the values of pd_0 and pd_t as in [19] to be used in the FES-driven tasks examples. These parameters characterize how sensitive the muscle is to the stimulation intensity. To achieve that, it would be necessary to evaluate stimulation with different pulse duration values, which was not taken into account in our experiments with subjects with SCI. Moreover, while the present study encompasses isometric and knee extension movements, the proposed model addresses neither the force-velocity relationship nor the fatigue effects within the model. In contrast, previous studies have incorporated the essential formulation to facilitate the estimation of dynamic movements as in [21], [22], and muscle fatigue under both isometric and non-isometric conditions [23]–[25]. Furthermore, although the biomechanical model incorporated four muscles, specific functions, such as maintaining balanced activation between the medio-lateral muscles, which is crucial to reducing the risk of joint injury, were not evaluated in the simulation. Finally, the FES-driven tasks presented in this work were not experimentally validated.

However, this preliminary evaluation employing a comprehensive musculoskeletal optimization-based motion prediction methodology, including the formulation of trajectory optimization problems, is a crucial step in the process of using physiological model-based control laws with embedded systems applications for real-time control, supporting the development of our proposed model to improve the FES-stimulation strategies. Also, the formulations obtained from studies conducted in non-isometric scenarios and incorporating muscle fatigue [25] can be leveraged to enhance the efficacy of our adapted model in simulating complex activities. Moreover, we can expect large improvements in computational performance by switching our approach to include real-time iteration algorithms such as the one implemented in ACADOS [37], thanks to which it was proven that real-time optimization of musculoskeletal simulations was feasible [38], [39]. Furthermore, we could take advantage of its ease of implementation and use approximation methods, such as the finite-dimensional approximation presented in [40], to investigate trajectory optimization in real-time applications. Although no details regarding its implementation in real-system were given, their methodology may facilitate the implementation of the model in FES-systems and, if associate with our adaptations, trajectory optimization could be further investigated.

Subsequent works will endeavor to enhance the model to account for muscle fatigue and the force-velocity relationships of muscle contractions, in addition to exploring the potential applications for real-time use. This improvement will enable our methodology to better understand the efficiency of FES-driven activities for people with SCI, such as in FES-assisted cycling or walking.

V. Conclusion

In this study, we adapted a physiological muscle model that is capable of predicting muscle force in response to electrical stimulation to make it compatible with gradient-based optimization. We demonstrated the potential of using this model with an optimal control framework to predict and control biomechanical tasks in simulation while maintaining the phenomenological approach behind muscle contractions. Our research contributes to the field by incorporating physiological knowledge of FES-stimulated muscle contractions in combination with musculoskeletal dynamics and numerical optimal control. Although not being a final solution, this is a fundamental step to improve the realism of simulations and to advance current abilities in devising optimal functional electrical stimulation protocols for complex movement tasks in real-world applications.

Acknowledgment

We thank M. Schmoll, R. Le Guillou and E. Fachin-Martins for allowing the use of the experimental data from [31].

References

[1] P. H. Hunter and J. S. Knutson, "Functional electrical stimulation for neuromuscular applications," *Annual review of biomedical engineering*, vol. 7, pp. 327–360, 2005, 10.1146/annurev.bioeng.6.040803.140103

[2] K. D. Atkins and C. S. Bickel, "Effects of functional electrical stimulation on muscle health after spinal cord injury," *Current Opinion in Pharmacology*, vol. 60, pp. 226–231, Oct. 2021, 10.1016/j.coph.2021.07.025

[3] F. De Groote, A. L. Kinney, A. V. Rao, and B. J. Fregly, "Evaluation of direct collocation optimal control problem formulations for solving the muscle redundancy problem," *Annals of Biomedical Engineering* vol. 44, pp. 2922–2936, Mar. 2016, 10.1007/s10439-016-1591-9

[4] N. Kirsch, N. Alibeji, and N. Sharma, "Nonlinear model predictive control of functional electrical stimulation," *Control Engineering Practice*, vol. 58, pp. 319–331, Jan. 2017, 10.1016/j.conengprac.2016.03.005

[5] D. Popović, R.B. Stein, N. Oğuztöreli, M. Lebiedowska, and S. Jonić, "Optimal control of walking with functional electrical stimulation: a computer simulation study," *IEEE transactions on rehabilitation engineering : a publication of the IEEE Engineering in Medicine and Biology Society*, vol. 7, no. 1, pp. 69—79, 1999, 10.1109/86.750554

[6] S. Dosen, and D.B. Popović, "Moving-window dynamic optimization: design of stimulation profiles for walking," *IEEE transactions on bio-medical engineering*, vol. 56, no. 5, pp. 1298-–1309, 1999, 10.1109/TBME.2009.2013935

[7] D. Popović, M. Radulović, L. Schwirtlich, and N. Jauković, "Automatic vs hand-controlled walking of paraplegics," *Medical engineering & physics*, vol. 25(1), pp. 63–73, 2003, 10.1016/s1350-4533(02)00188-1

[8] V. Nekoukar, and A. Erfanian, "Dynamic optimization of walker-assisted FES-activated paraplegic walking: Simulation and experimental studies," *Medical Engineering & Physics*, vol. 35, no. 11, pp. 1659—1668, 2013, 10.1016/j.medengphy.2013.06.001

[9] N. Dunkelberger, S. A. Carlson, J. Berning, E. M. Schearer, and M. K. O'Malley, "Multi Degree of Freedom Hybrid FES and Robotic Control of the Upper Limb," *IEEE transactions on neural systems and rehabilitation engineering : a publication of the IEEE Engineering in Medicine and Biology Society*, vol. 32, pp. 956–966, 2024, 10.1109/TNSRE.2024.3364517

[10] N. Dunkelberger, J. Berning, E. M. Schearer, and M. K. O'Malley, "Hybrid FES-exoskeleton control: Using MPC to distribute actuation for elbow and wrist movements," *Frontiers in Neurorobotics*, vol. 17, 2023, DOI=10.3389/fnbot.2023.1127783

[11] D. N. Wolf, A. J. van den Bogert, and E. M. Schearer, "Data-Driven Dynamic Motion Planning for Practical FES-Controlled Reaching Motions in Spinal Cord Injury," *IEEE transactions on neural systems and rehabilitation engineering : a publication of the IEEE Engineering in Medicine and Biology Society*, vol. 31, pp. 2246–2256, 2023, 10.1109/TNSRE.2023.3272929

[12] L.A. Frey Law, and R.K. Shields, "Mathematical models of human paralyzed muscle after long-term training," *Journal of Biomechanics*, vol. 40, no. 12, pp. 2587–2595, 2007, 10.1016/j.jbiomech.2006.12.015

[13] J. Ding, S. A. Binder-Macleod S A, and A. S. Wexler, "Two-step, predictive, isometric force model tested on data from human and rat muscles," *Journal of applied physiology (Bethesda, Md. : 1985)*, vol. 85, no. 6, pp. 2176–2189, Dec. 1998, 10.1152/jappl.1998.85.6.2176

[14] J. Ding, A. S. Wexler, and S. A. Binder-Macleod, "A mathematical model that predicts the force-frequency relationship of human skeletal muscle," *Muscle Nerve*, vol. 26, no. 4, pp. 477–485, Oct. 2002, 10.1002/mus.10198

[15] J. Ding, A. S. Wexler, and S. A. Binder-Macleod, "Mathematical models for fatigue minimization during functional electrical stimulation," *Journal of Electromyography and Kinesiology*, vol. 13, no. 6, pp. 575–588, Dec. 2003, 10.1016/S1050-6411(03)00102-0

[16] P.R. Shorten, P. O'Callaghan, J. B. Davidson, and T. K. Soboleva, "A mathematical model of fatigue in skeletal muscle force contraction," *Journal of Muscle Research and Cell Motility*, vol. 28, pp. 293–313, 2007, doi.org/10.1007/s10974-007-9125-6

[17] H. El Makssoud, D. Guiraud, P. Poignet, M. Hayashibe, P. Wieber, K. Yoshida, and C. Azevedo-Coste, "Multiscale modeling of skeletal muscle properties and experimental validations in isometric conditions," *Biological Cybernetics*, vol. 105, pp. 121–138, 2011, 10.1007/s00422-011-0445-7

[18] J. Ding, S. C. K. Lee, T. E. Johnston and A. S. Wexler, W. B. Scott, and S. A. Binder-Macleod, "Mathematical model that predicts isometric muscle forces for individuals with spinal cord injuries," *Muscle &amp Nerve*, vol. 31, no. 6, pp. 702–712, Mar. 2005, 10.1002/mus.20303.

[19] J. Ding, Li-Wei Chou, T. M. Kesar, S. C. K. Lee, T. E. Johnston, and A. S. Wexler, and S. A. Binder-Macleod, "Mathematical model that predicts the force–intensity and force–frequency relationships after spinal cord injuries," *Muscle Nerve*, vol. 36, no. 2, pp. 214–222, Aug. 2007, 10.1002/mus.20806.

[20] L.A. Frey Law, and R.K. Shields, "Predicting human chronically paralyzed muscle force: a comparison of three mathematical models," *Journal of Applied Physiology*, vol. 100, no. 3, pp. 1027–1036, 2006, 10.1152/japplphysiol.00935.2005

[21] R. Perumal, A. S. Wexler, and S. A. Binder-Macleod, "Mathematical model that predicts lower leg motion in response to electrical stimulation," *Journal of Biomechanics*, vol. 39, no. 15, Nov. 2005, 10.1016/j.jbiomech.2005.09.021

[22] R. Perumal, A. S. Wexler, and S. A. Binder-Macleod, "Development of a mathematical model for predicting electrically elicited quadriceps femoris muscle forces during isovelocity knee joint motion," *Journal of NeuroEngineering and Rehabilitation*, vol. 5, no. 33, 2008, 10.1186/1743-0003-5-33

[23] M. S. Marion, A. S. Wexler, M. L. Hull, and S. A. Binder-Macleod, "Predicting the effect of muscle length on fatigue during electrical stimulation," *Muscle Nerve*, vol. 40, no. 4, pp. 573-581, Oct. 2009, 10.1002/mus.21459

[24] M. S. Marion, A. S. Wexler, and M. L. Hull, "Predicting fatigue during electrically stimulated non-isometric contractions," *Muscle Nerve*, vol. 41, no. 6, pp. 857-867, Jun. 2010, 10.1002/mus.21603

[25] M. S. Marion, A. S. Wexler, and M. L. Hull, "Predicting non-isometric fatigue induced by electrical stimulation pulse trains as a function of pulse duration," *Journal of NeuroEngineering and Rehabilitation*, vol. 10, no. 13, Feb. 2013, 10.1186/1743-0003-10-13

[26] T. Bakir, B. Bonnard, and J. Rouot, "A case study of optimal input-output system with sampled-data control: Ding et al. force and fatigue muscular control model," *Networks and Heterogeneous Media*, vol. 14, no. 1, pp. 79–100, Jan. 2019, 10.3934/nhm.2019005

[27] B, Bonnard, and J. Rouot, "Geometric optimal techniques to control the muscular force response to functional electrical stimulation using a non-isometric force-fatigue model," *Journal of Geometric Mechanics*, vol. 13, no. 1, pp. 1–23, Mar. 2021, 10.3934/jgm.2020032

[28] B. D. Doll, N. A. Kirsch, X. Bao, B. E. D, and N. Sharma, "Dynamic optimization of stimulation frequency to reduce isometric muscle fatigue using a modified Hill-Huxley model," *Muscle Nerve*, vol. 57, no. 4, pp. 634–641, Apr. 2018, 10.1002/mus.25777

[29] P. Puchaud, F. Bailly and M. Begon, "Direct multiple shooting and direct collocation perform similarly in biomechanical predictive simulations," *Computer Methods in Applied Mechanics and Engineering*, 414, 116162, 2023.

[30] R. Perumal, A. S. Wexler, J. Ding, and S. A. Binder-Macleod, "Modeling the length dependence of isometric force in human quadriceps muscles," *Journal of Biomechanics*, vol. 35, no. 7, pp. 919–930, Jul. 2002, 10.1016/s0021-9290(02)00049-0

[31] M. Schmoll, R. Le Guillou, D. L. Borges, C. Fattal, E. Fachin-Martins, and C. A. Coste, "Standardizing fatigue-resistance testing during electrical stimulation of paralysed human quadriceps muscles, a practical approach," *Journal of Neuroengineering and Rehabilitation*, vol. 18, no. 1:11, Jan. 2021, 10.1186/s12984-021-00805-7

[32] B. Michaud, F. Bailly, E. Charbonneau, A. Ceglia, L. Sanchez, and M. Begon, "Bioptim, a Python framework for musculoskeletal optimal control in biomechanics," *IEEE Transactions on Systems, Man, and Cybernetics: Systems*, vol. 53, no. 1, pp. 321–332, Jun. 2022, 10.1109/TSMC.2022.3183831

[33] A. Wächter, and L.T. Biegler, "On the implementation of an interior-point filter line-search algorithm for large-scale nonlinear programming," *Mathematical Programming*, vol. 106, pp. 25–57, 2006, 10.1007/s10107-004-0559-y

[34] J.A.E. Andersson, J. Gillis, G. Horn, J.B. Rawlings, and M. Diehl, "CasADi: a software framework for nonlinear optimization and optimal control," *Mathematical Programming Computation*, vol. 11, pp. 1–36, 2019, 10.1007/s12532-018-0139-4

[35] M. O. Ibitoye, N. A. Hamzaid, N. Hasnan, A. K. A. Wahab, and G. M. Davis, "Strategies for rapid muscle fatigue reduction during FES exercise in individuals with spinal cord injury: a systematic Review," *PLOS ONE*, vol.11, no. 2:e0149024, 2016, 10.1371/journal.pone.0149024

[36] A. B. Hmed, T. Bakir, A. Sakly and S. Binczak, "A new mathematical force model that predicts the force-pulse amplitude relationship of human skeletal muscle," *2018 40th Annual International Conference of the IEEE Engineering in Medicine and Biology Society (EMBC)*, Honolulu, HI, USA, 2018, pp. 3485-3488, 10.1109/EMBC.2018.8512946

[37] R. Verschueren, G. Frison, D. Kouzoupis, J. Frey, N. van Duijkeren, A. Zanelli, B. Novoselnik, T. Albin, R. Quirynen, and M. Diehl, "Acados—a modular open-source framework for fast embedded optimal control," *Mathematical Programming Computation*, vol. 14, pp. 147–183, 2022, 10.1007/s12532-021-00208-8

[38] F. Bailly, A. Ceglia, B. Michaud, D. M. Rouleau, and M. Begon, "Real-time and dynamically consistent estimation of muscle forces using a moving horizon EMG-marker tracking algorithm—application to upper limb biomechanics," *Frontiers in bioengineering and biotechnology*, vol. 9, no. 642742, Fev. 2021, 10.3389/fbioe.2021.642742

[39] A. Ceglia, F. Bailly and M. Begon, "Moving horizon estimation of human kinematics and muscle forces," *IEEE Robotics and Automation Letters*, vol. 8, no. 8, pp. 5212-5219, 2023, 10.1109/LRA.2023.3291921

[40] T. Bakir, B. Bonnard, S. Gayrard, and J. Rouot, "Finite dimensional approximation to muscular response in force-fatigue dynamics using functional electrical stimulation," *Automatica*, vol. 144, no. 110464, Oct. 2022, 10.1016/j.automatica.2022.110464